Determination of Cole–Cole parameters using only the real part of electrical impedivity measurements

2008 Physiol. Meas. 29 669

(http://iopscience.iop.org/0967-3334/29/5/011)

IOP PUBLISHING PHYSIOLOGICAL MEASUREMENT

Physiol. Meas. **29** (2008) 669–683 doi:10.1088/0967-3334/29/5/011

Determination of Cole–Cole parameters using only the real part of electrical impedivity measurements

David A Miranda[1] **and S A López Rivera**[2]

[1] CIMBIOS, Universidad Industrial de Santander, Bucaramanga Cr27-Cll9, Colombia
[2] Laboratorio de Física Aplicada, Universidad de los Andes, Mérida, Venezuela

E-mail: dalemir@uis.edu.co and adan@ula.ve

Received 30 January 2008, accepted for publication 1 April 2008
Published 7 May 2008
Online at stacks.iop.org/PM/29/669

Abstract
An algorithm is presented to determine the Cole–Cole parameters of electrical impedivity using only measurements of its real part. The algorithm is based on two multi-fold direct inversion methods for the Cole–Cole and Debye equations, respectively, and a genetic algorithm for the optimization of the mean square error between experimental and calculated data. The algorithm has been developed to obtain the Cole–Cole parameters from experimental data, which were used to screen cervical intra-epithelial neoplasia. The proposed algorithm was compared with different numerical integrations of the Kramers–Kronig relation and the result shows that this algorithm is the best. A high immunity to noise was obtained.

Keywords: bioelectrical impedance analysis, Cole–Cole model, neoplasical screening, geophysics and material science, Cole–Cole fitting

1. Introduction

The impedivity is the complex electrical resistivity as dependent on the frequency. Some researchers call it electrical impedance spectrum, but this name does not consider its unit, ohm meter (electrical resistivity units). This reason suggests the use of the term impedivity, proposed by Brown *et al*, to reference the complex electrical resistivity.

There has been considerable interest in the use of electrical resistivity spectra for many applications, e.g. neoplasical screening, electrical bioimpedance and geophysics (Brown *et al* 2000, Xiang *et al* 2003). The spectral-induced polarization (SIP) technique is a kind of electromagnetic exploration method in a frequency domain. This method is widely used in environmental studies and engineering exploration methods, geophysics, oil, gas and coal explorations (Cao *et al* 2005). In the theory of the interpretation of these spectra, the Cole–Cole model is a basic expression. There are available techniques for measuring the real part,

the amplitude, the phase and the imaginary part of impedivity (Xiang *et al* 2003, Ackmann and Seitz 1984), but some research groups (Brown *et al* 2000, Miranda *et al* 2007) only measure the real part of the spectrum, since experimental errors are less when only recording this one. A new algorithm is presented to search the imaginary part of the impedivity from the real part. This algorithm enables the fitted experimental data to determine the important Cole–Cole parameters using only the real part of the impedivity.

2. Mathematical model to analyze the impedivity spectrum

The use of models such as Cole–Cole for characterizing experimental data is common, but the algorithms for inverting the equations require both the real and imaginary parts of the impedance, e.g. Xiang *et al* (2003) and Ward *et al* (2006).

The complex electrical impedivity expression of the Cole–Cole equation (Cole 1940, Cole and Cole 1941) is written as

$$\rho = \rho_\infty + \frac{\rho_o - \rho_\infty}{1 + (\mathrm{j}\omega\tau)^{1-\alpha}} = \rho_o \left\{1 - m\left[1 - \frac{1}{1 + (\mathrm{j}\omega\tau)^c}\right]\right\}, \quad \text{and} \quad \begin{cases}\alpha = 1 - c \\ \rho_\infty = \rho_o(1 - m),\end{cases} \tag{1}$$

where ρ_∞ is the high-frequency resistivity, ρ_o is the low-frequency resistivity, τ is the central relaxation time, α or c is the dispersion parameter, and m is the polarizability.

Kramers and Kronig demonstrated that the imaginary part of the electrical permittivity is absolutely defined if the real part is known (Xiang *et al* 2001, Kronig 1926, Kramers 1927), but it is necessary to know the real part of the spectrum for all frequencies. The Kramers–Kronig relations could be extended to the complex electrical resistivity (or electrical impedivity). The numerical integration for the Kramers–Kronig relations is shown for two different methods in the numeral six. To show the advantage of the proposed method in this paper, the result of the three different methods is compared in the numeral seven.

A new technique is proposed to obtain the Cole–Cole parameters from the real part of an electrical impedivity spectrum, with access to finite data. The basic procedure is described as follows: first, a direct inversion method is used to obtain the parameters of the Debye models and to calculate an approximation for the imaginary part of the spectrum. Second, Xiang's algorithm (Xiang *et al* 2003, 2001) is used to invert the electrical resistivity spectrum formed from experimental data and the imaginary part obtained in the first step. Third, the Cole–Cole parameters obtained with the Xiang algorithm and the relaxation time of the Debye model are used to calculate the electrical impedivity spectrum. Finally, a genetic algorithm is used to minimize the root mean square error between experimental data and the Cole–Cole equation.

3. The direct inversion of the Debye model

The Debye model is inverted (equation (1) with $\alpha = 0$, or $c = 1$). From the experimental data, ρ_0, m and τ are estimated. Assuming the data as $\{(\omega_k, R_k)|k = 1, 2, \ldots, N + 1\}$, where $R_k = \mathrm{Re}\{\rho(\mathrm{j}\omega_k)\}$, $k = 1, 2, \ldots, N + 1$, the Debye model gives the relations

$$R_k = \rho_\infty + \frac{\rho_0 - \rho_\infty}{1 + (\omega_k\tau)^2} \tag{2}$$

$$R_k - \rho_0 = \left(-R_k\omega_k^2 + \rho_\infty\omega_k^2\right)\tau^2. \tag{3}$$

Estimating $\frac{R_k - R_{k+1}}{R_{k-1} - R_k}$, $x = \rho_\infty$, and using (2) and (3), it can be obtained as

$$\frac{R_k - R_{k+1}}{R_{k-1} - R_k} = \frac{-R_k\omega_k^2 + x\omega_k^2 + R_{k+1}\omega_{k+1}^2 - x\omega_{k+1}^2}{-R_{k-1}\omega_{k-1}^2 + x\omega_{k-1}^2 + R_k\omega_k^2 - x\omega_k^2}. \tag{4}$$

By reordering the terms it is possible to write (4) as $A_{\infty k}x = B_{\infty k}$, where

$$\begin{aligned} A_{\infty k} &= (R_{k+1} - R_k)\,\omega_{k-1}^2 - (R_{k+1} - R_{k-1})\,\omega_k^2 - (R_k - R_{k-1})\,\omega_{k+1}^2 \\ B_{\infty k} &= (R_{k+1} - R_k)\,R_{k-1}\omega_{k-1}^2 - (R_{k+1} - R_{k-1})\,R_k\omega_k^2 - (R_k - R_{k-1})\,R_{k+1}\omega_{k+1}^2. \end{aligned} \tag{5}$$

Then, using the least-square approximation to minimize the mean quadratic error, $s_x = \frac{1}{N+1}\sum_k (A_{\infty k}x - B_{\infty k})^2$, it is obtained as

$$\rho_\infty = \frac{\sum_{k=1}^N A_{\infty k}B_{\infty k}}{\sum_{k=1}^N A_{\infty k}^2}. \tag{6}$$

To find ρ_0 it is necessary to resolve $\frac{R_k - R_{k+1}}{\rho_0 - R_k}$, using (2) and (3) and $y = \rho_0$, and the least-square approximation is calculated in order to minimize the mean quadratic error $s_y = \frac{1}{N+1}\sum_k (A_{0k}y - B_{0k})^2$:

$$\begin{aligned} A_{0k} &= (R_{k+1} - R_\infty)\omega_{k+1}^2 - (R_k - R_\infty)\omega_k^2 \\ B_{0k} &= (R_{k+1} - R_\infty)R_k\omega_{k+1}^2 - (R_k - R_\infty)R_{k+1}\omega_k^2 \end{aligned} \tag{7}$$

$$\rho_0 = \frac{\sum_{k=1}^N A_{0k}B_{0k}}{\sum_{k=1}^N A_{0k}^2}. \tag{8}$$

Equations (3) and (6) allow us to obtain the parameter τ. First, $z = \tau^2$, $J_k = \rho_\infty\omega_k^2 - R_k\omega_k^2$ and $L_k = R_k - \rho_0$, and second, $J_k z = L_k$. Using the least-square approximation to minimize the mean quadratic error $s_z = \frac{1}{N+1}\sum_k (J_k z - L_k)^2$ it is found that

$$\tau = \sqrt{\frac{\sum_{k=1}^{N+1} J_k L_k}{\sum_{k=1}^{N+1} J_k^2}}. \tag{9}$$

4. Xiang inversion and the optimization problem

Once the Debye parameters are obtained, an approximation for the imaginary part of ρ for each frequency can be calculated using

$$I_k = -\frac{(\rho_0 - \rho_\infty)\,\omega_k\tau}{1 + \omega_k^2\tau^2}. \tag{10}$$

The impedivity is defined as $\rho_k = R_k + \mathrm{j}I_k$ and the Cole–Cole parameters: $\rho_0^{(0)}$, $m^{(0)}$, $\alpha^{(0)}$ and $\tau^{(0)}$ are estimated using the Xiang (Xiang *et al* 2001) inversion technique.

In order to obtain more accurate values for the parameters from the Cole–Cole equation when fitted to the experimental data, an optimization of the root mean square error (12) can be used through step (11). To implement the optimization of the root mean square error (12), it is necessary to use a non-classical technique, a genetic algorithm, because equation (12) has many local minima and only one global minimum. The minimization of (12) through the path (11) is proposed:

$$\begin{aligned} \tau^{(k+1)} &= p_1^{(k)}\tau^{(0)} + q_1^{(k)} & \rho_0^{(k+1)} &= p_2^{(k)}\rho_0^{(0)} + q_2^{(k)} \\ \rho_\infty^{(k+1)} &= p_3^{(k)}\rho_\infty^{(0)} + q_3^{(k)} & \alpha^{(k+1)} &= p_4^{(k)}\alpha^{(0)} + q_4^{(k)} \end{aligned} \tag{11}$$

$$\mathrm{Err} = \sqrt{\frac{1}{N+1}\sum_k (R_k - \mathrm{Re}\{\rho_k\}_{\mathrm{Calculated}})^2}, \tag{12}$$

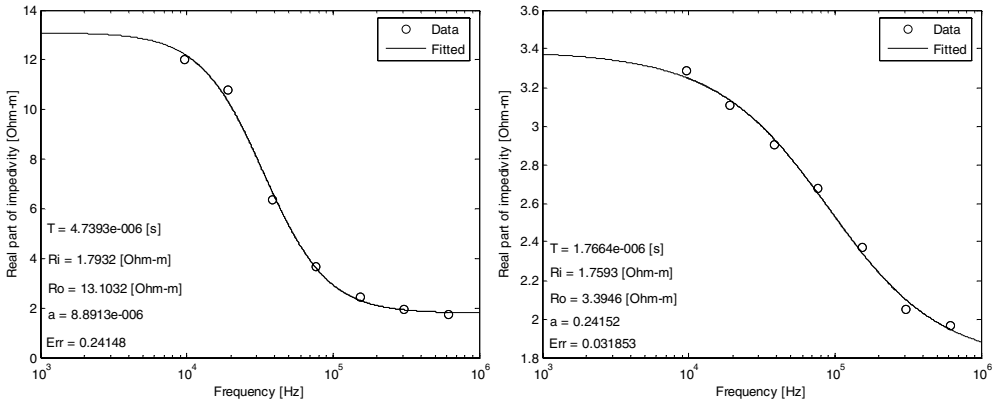

Figure 1. Two examples of the measurements and fitting of real part of electrical impedivity. This figure shows data for (a) normal cervical tissue and (b) invasive cervical carcinoma.

where $p_1^{(k)}, p_2^{(k)}, p_3^{(k)}, p_4^{(k)}, q_1^{(k)}, q_2^{(k)}, q_3^{(k)}$ and $q_4^{(k)}, k = 1, 2, \ldots$ are genetic algorithm searching parameters. The parameter $\tau^{(0)}$ used in equation (11) is calculated with the Debye direct inversion, equation (9), the other parameters are obtained by the Xiang inversion method.

5. Algorithm and numerical examples

The parameters of the Cole–Cole model and the imaginary part of the impedance may be investigated based on the methods of the previous sections. The algorithm is described as follows: first, equations (5)–(9) are used to get the Debye parameters ρ_0, ρ_∞ and τ; second, equation (10) is used to calculate the first approximation of the imaginary part of impedance; third, the real part of impedance (data) and the first approximation of the imaginary part (calculated in the second step) are used to approximate the Cole–Cole parameters $\alpha^{(0)}$, $\rho_0^{(0)}$, $\rho_\infty^{(0)}$ and $\tau^{(0)}$by the Xiang algorithm (Xiang *et al* 2001). The final step is to search the Cole–Cole parameters α, ρ_0, ρ_∞ and τ with a genetic algorithm to minimize the root mean square error (12) through the steps shown in (11).

The above algorithm was implemented as a Matlab function. Here four examples of the use of these algorithms are presented to show the utility and accuracy of this method.

5.1. Medical application of the impedivity in cervical tissue

Many measurements of the impedivity were made in patients in the hospital of the Santander University. Figure 1 shows some typical results of the adjusted electrical resistivity real part spectrum of cervical tissue; the four important calculated parameters are shown inside the figure. The measurements were made using the MARK III system of Sheffield University and a tetrapolar probe (Miranda *et al* 2007). As shown in figure 1, the Cole–Cole parameters are significantly different for the normal cervical tissue and for an invasive cervical carcinoma.

5.2. Bioimpedance of neoplasical cervical tissue

The impedivity is used to investigate different properties of tissues, such as neoplasical tissues. In the neoplasical tissue studies, the impedivity was measured in the β dispersion zone

(10^3 Hz $< f <$ 10^6 Hz) (Brown *et al* 2000, Schwan 1994). Using a given set of Cole–Cole parameters for neoplasical cervical tissue obtained from Miranda *et al* (2007),

$$\tau = 1.8 \times 10^{-6}\ (\mathrm{s}), \qquad \rho_0 = 3.24\ (\Omega\,\mathrm{m}), \qquad \rho_\infty = 1.34\ (\Omega\,\mathrm{m}) \wedge \alpha = 0.31.$$

The real part of the impedivity is calculated and the proposed algorithm is used to obtain the imaginary part of the impedivity and the Cole–Cole parameters. Before the implementation of the algorithm it is necessary to calculate the real part of the impedivity using (2), some frequency values and the given Cole–Cole parameters:

$$\omega = 2\pi\{100, 464.16, 2154.40, 10^4, 46\,416, 215\,440, 10^6\}\ (\mathrm{rad\ s^{-1}})$$
$$R = \{3.2317, 3.2155, 3.166, 3.0082, 2.5683, 1.9164, 1.5329\}\ (\Omega\,\mathrm{m})$$

The implementation of the algorithm is presented as follows. First, the Debye parameters are calculated using equations (5)–(9):

$$\tau = 9.9814 \times 10^{-7}\ (\mathrm{s})$$
$$\rho_0 = 2.6669\ (\Omega\,\mathrm{m})$$
$$\rho_\infty = 1.5042\ (\Omega\,\mathrm{m}).$$

Second, the first approximation of the imaginary part of the impedivity is calculated using (10):

$$I = \{-0.000\,729, -0.003\,385, -0.015\,707, -0.072\,632, -0.312\,02, -0.555\,98, -0.1808\}\ (\Omega\,\mathrm{m}).$$

Third, taking R, I and the Xiang algorithm, the first approximation of the Cole–Cole parameters is calculated:

$$\tau^{(0)} = 1.8299 \times 10^{-48}\ (\mathrm{s})$$
$$\rho_0^{(0)} = 3.2408\ (\Omega\,\mathrm{m})$$
$$\rho_\infty^{(0)} = 1.2386\ (\Omega\,\mathrm{m})$$
$$\alpha^{(0)} = 0.320\,36.$$

Fourth, a genetic algorithm is defined with the following parameters: generations = 100, fitness limit = 10^{-4}, stall genetic limit = infinite, stall time limit = infinite, crossover fraction = 0.6, elite count = 20, migration direction = both, migration fraction = 0.4, migration interval = 5, population size = 5000 and the population initial range = [0, 1]. The genetic algorithm minimized the error (12) through step (11):

$$\tau^{(0)} = 1.7866 \times 10^{-6}\ (\mathrm{s})$$
$$\rho_0^{(0)} = 3.2406\ (\Omega\,\mathrm{m})$$
$$\rho_\infty^{(0)} = 1.3346\ (\Omega\,\mathrm{m})$$
$$\alpha^{(0)} = 0.3124.$$

Fifth, equation (1) is used to get the imaginary part of the impedivity. Figure 2 shows the impedivity:

$$I = -\{0.0154, 0.0437, 0.1200, 0.2968, 0.5353, 0.5049, 0.2601\}\ (\Omega\,\mathrm{m}).$$

The above algorithm may use different sets of impedivity data and different values for the generations of a genetic algorithm. Table 1 presents the results using different sets of impedivity data and different values of generations.

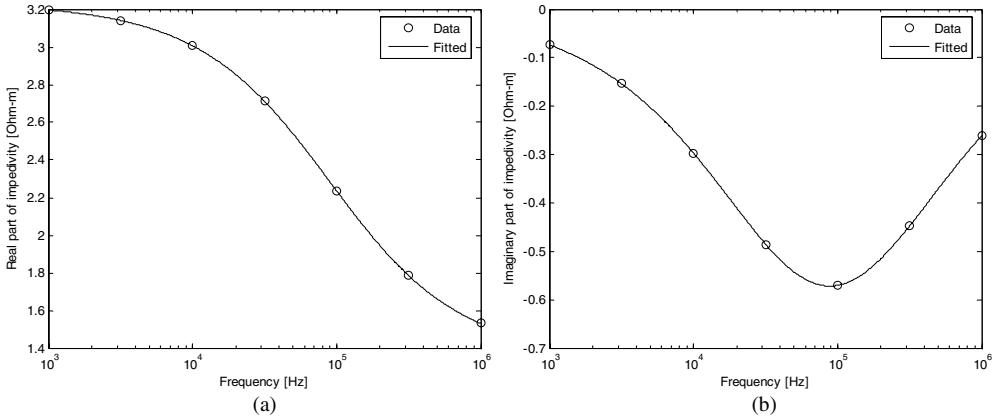

Figure 2. (a) Real and (b) imaginary parts of the impedivity of cervical neoplasical tissue.

Table 1. Results for bioimpedance of cervical neoplasical tissue.

The number of spectral data	Generations	τ (μs)	ρ_0 (Ω m)	ρ_∞ (Ω m)	α
5	10	1.84	3.2330	1.3408	0.31009
5	100	1.80	3.2397	1.3415	0.30932
5	880	1.80	3.2399	1.3405	0.30972
7	10	1.76	3.2261	1.3432	0.30219
7	100	1.80	3.2405	1.3378	0.31196
7	880	1.80	3.2398	1.3406	0.30967
10	10	1.43	3.2249	1.2446	0.32632
10	100	1.78	3.2418	1.3299	0.31412

5.3. Estimation of Cole–Cole parameters and comparison with Jaggar and Xiang inversion models

Table 2 presents a set of impedivity data obtained from Jaggar and Fell (1988). From this table the Cole–Cole parameters can be calculated. To estimate the Cole–Cole parameters, it is necessary to take the real part of the impedivity (the fourth column of table 2). The implementation of the algorithm for a set of nine data of the real part impedivity is presented as follows:

$$\omega = 2\pi\{0.022, 0.100, 0.464, 2.154, 10.00, 46.42, 215.40, 1000, 4642\}\ (\text{rad s}^{-1})$$

$$\text{Re}\{\rho\ (\text{j}\omega)\} = \{21.990, 21.980, 21.960, 21.910, 21.717, 21.229, 20.345, 19.601, 19.270\}\ (\Omega\,\text{m}).$$

First, the Debye parameters are calculated using equations (5)–(9):

$$\tau = 2.56019 \times 10^{-4}\ (\text{s}),$$
$$\rho_0 = 20.503\,25\ (\Omega\,\text{m}), \qquad \rho_\infty = 19.248\,09\ (\Omega\,\text{m}).$$

Second, the first approximation of the imaginary part of the impedivity is calculated using (10):

$$I = \left\{ \begin{matrix} -0.000\,043, -0.000\,202, -0.000\,937, -0.004\,349, -0.020\,186, \\ -0.093\,206, -0.388\,290, -0.562\,790, -0.165\,130 \end{matrix} \right\}\ (\Omega\,\text{m}).$$

Table 2. Field data from Jaggar and Fell (1988).

Frequency (Hz)	Amplitude (Ω m)	Phase (mrad)	Real part (Ω m)	Imaginary part (Ω m)
1.000×10^{-2}	2.200×10^{1}	0.000×10^{0}	2.200×10^{1}	0.000×10^{0}
2.154×10^{-2}	2.199×10^{1}	0.000×10^{0}	2.199×10^{1}	0.000×10^{0}
4.642×10^{-2}	2.197×10^{1}	0.000×10^{0}	2.197×10^{1}	0.000×10^{0}
1.000×10^{-1}	2.198×10^{1}	0.000×10^{0}	2.198×10^{1}	0.000×10^{0}
2.150×10^{-1}	2.197×10^{1}	0.000×10^{0}	2.197×10^{1}	0.000×10^{0}
4.640×10^{-1}	2.196×10^{1}	-1.52×10^{0}	2.196×10^{1}	-3.338×10^{-2}
1.000×10^{0}	2.195×10^{1}	-3.36×10^{0}	2.195×10^{1}	-7.375×10^{-2}
2.154×10^{0}	2.191×10^{1}	-6.11×10^{0}	2.191×10^{1}	-1.339×10^{-1}
4.642×10^{0}	2.184×10^{1}	-1.049×10^{1}	2.184×10^{1}	-2.291×10^{-1}
1.000×10^{1}	2.172×10^{1}	-1.637×10^{1}	2.172×10^{1}	-3.555×10^{-1}
2.154×10^{1}	2.154×10^{1}	-2.483×10^{1}	2.153×10^{1}	-5.348×10^{-1}
4.642×10^{1}	2.124×10^{1}	-3.248×10^{1}	2.123×10^{1}	-6.898×10^{-1}
1.000×10^{2}	2.083×10^{1}	-4.014×10^{1}	2.081×10^{1}	-8.359×10^{-1}
2.154×10^{2}	2.036×10^{1}	-3.856×10^{1}	2.035×10^{1}	-7.849×10^{-1}
4.642×10^{2}	1.996×10^{1}	-3.319×10^{1}	1.995×10^{1}	-6.624×10^{-1}
1.000×10^{3}	1.961×10^{1}	-2.953×10^{1}	1.960×10^{1}	-5.790×10^{-1}
2.154×10^{3}	1.940×10^{1}	-1.746×10^{1}	1.940×10^{1}	-3.387×10^{-1}
4.642×10^{3}	1.927×10^{1}	-1.980×10^{0}	1.927×10^{1}	-3.816×10^{-2}
1.000×10^{4}	1.884×10^{1}	-7.930×10^{0}	1.884×10^{1}	-1.494×10^{-1}

Third, taking R, I and the Xiang algorithm, the first approximation of the Cole–Cole parameters is calculated:

$$\tau^{(0)} = 9.008\,22 \times 10^{-46}\ (\mathrm{s})$$
$$\rho_0^{(0)} = 21.9973\ (\Omega\,\mathrm{m})$$
$$\rho_\infty^{(0)} = 18.8264\ (\Omega\,\mathrm{m})$$
$$\alpha^{(0)} = 0.451\,89.$$

Fourth, a genetic algorithm is defined with the following parameters: generations = 100, fitness limit = 10^{-4}, stall genetic limit = infinite, stall time limit = infinite, crossover fraction = 0.6, elite count = 20, migration direction = both, migration fraction = 0.4, migration interval = 5, population size = 5000 and the population initial range = [0, 1]. The genetic algorithm minimized the error (12) through step (11).

$$\tau^{(0)} = 9.8542 \times 10^{-4}\ (\mathrm{s})$$
$$\rho_0^{(0)} = 22.0053\ (\Omega\,\mathrm{m})$$
$$\rho_\infty^{(0)} = 19.0548\ (\Omega\,\mathrm{m})$$
$$\alpha^{(0)} = 0.3659.$$

Fifth, equation (1) is used to get the imaginary part of the impedivity. Figure 3 shows the impedivity.

$$I = \left\{ \begin{matrix} -0.008\,615, -0.022\,661, -0.058\,967, -0.149\,190, -0.349\,070, \\ -0.661\,110, -0.793\,460, -0.540\,750, -0.257\,530 \end{matrix} \right\}\ (\Omega\,\mathrm{m})$$

The above algorithm may use different sets of impedivity data. Table 3 presents the results using different sets of impedivity data and compares the three models: Jaggar–Fell (1988),

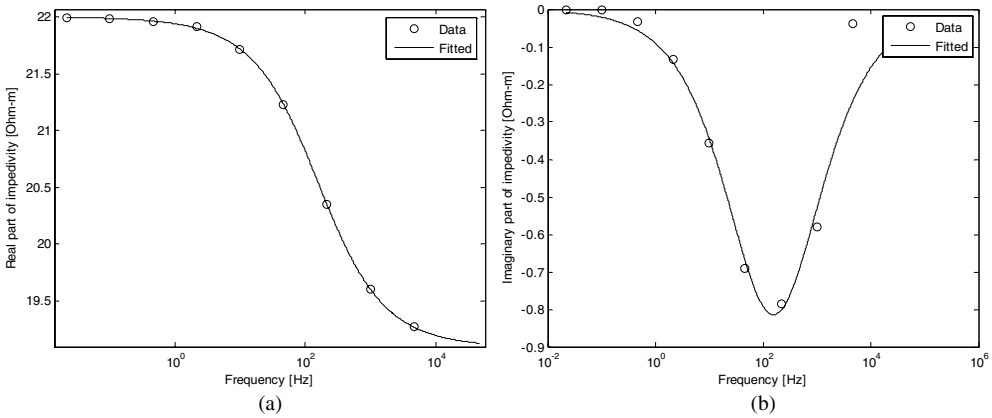

Figure 3. (a) Real and (b) imaginary parts of the impedivity using inversion for $N = 6$.

Table 3. Estimated parameters and a comparison of model by overall error.

Model	τ (s)	ρ_0 (Ω m)	m	c	Overall error
Jaggar-Fell, $N = 19$[a]	1.1000×10^{-3}	21.9	0.1300	0.7000	0.3164
Xiang inversion $N = 13$[a]	1.0000×10^{-3}	21.994	0.1343	0.6702	0.1684
Xiang inversion $N = 15$[a]	1.2000×10^{-3}	21.9902	0.1226	0.6824	0.3595
Xiang inversion $N = 17$[a]	8.1710×10^{-4}	21.9907	0.1373	0.6502	0.1930
Miranda inversion $N = 4$	1.7835×10^{-3}	21.975	0.1193	0.8604	0.9420
Miranda inversion $N = 5$	1.0317×10^{-3}	21.984	0.1300	0.6701	0.1932
Miranda inversion $N = 6$	9.8101×10^{-4}	21.999	0.1338	0.6431	0.1725
Miranda inversion $N = 7$	1.0662×10^{-3}	21.988	0.1303	0.6752	0.1882
Miranda inversion $N = 9$	9.8542×10^{-4}	22.005	0.1341	0.6340	0.1790
Miranda inversion $N = 10$	9.9264×10^{-4}	21.994	0.1321	0.6439	0.1899
Miranda inversion $N = 11$	9.8678×10^{-4}	21.997	0.1327	0.6441	0.1842
Miranda inversion $N = 13$	9.8103×10^{-4}	21.998	0.1330	0.6427	0.1821
Miranda inversion $N = 15$	9.9497×10^{-4}	21.997	0.1327	0.6434	0.1827
Miranda inversion $N = 16$	9.9953×10^{-4}	22.002	0.1329	0.6428	0.1834
Miranda inversion $N = 17$	9.9008×10^{-4}	22.001	0.1330	0.6421	0.1832
Miranda inversion $N = 18$	1.0261×10^{-3}	21.996	0.1314	0.6541	0.1894

[a] Data from Xiang *et al* (2003).

Xiang and the proposed model. The overall error was calculated as $\sum_k |R_k - \rho(j\omega_k)|^2$. The values of Xiang inversion and Jaggar–Fell were obtained from Xiang *et al* (2001). Table 3 shows a low variability of the Cole–Cole parameter and an overall error with respect to the data set number for the Miranda inversion.

5.4. Bioimpedance of normal cervical tissue

Using a given set of Cole–Cole parameters for normal cervical tissue obtained from Miranda *et al* (2007),

$\tau = 5.4 \times 10^{-6}$ (s), $\rho_0 = 14.25$ (Ω m), $\rho_\infty = 1.98$ (Ω m) and $\alpha = 0.14$.

The real part of the impedivity is calculated and the proposed algorithm is used to obtain the imaginary part of the impedivity and the Cole–Cole parameters.

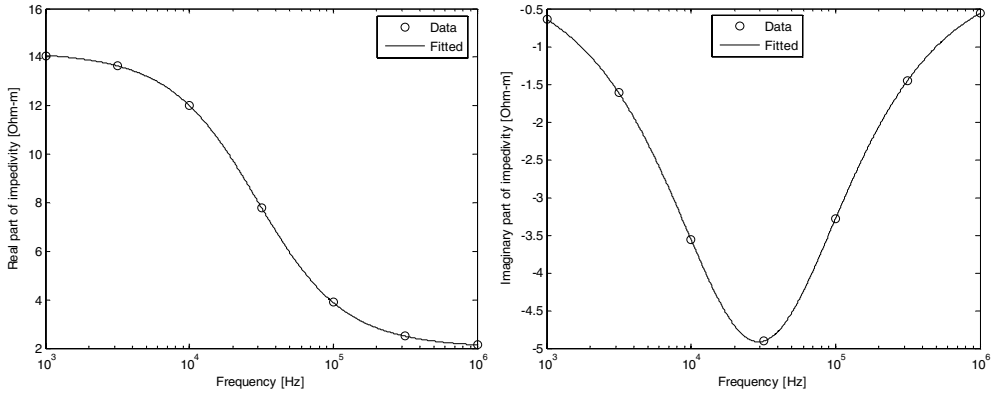

Figure 4. (a) Real and (b) imaginary parts of the impedivity for bioimpedance of normal cervical tissue.

Table 4. Results for bioimpedance of normal cervical tissue.

Number of spectral data	Generations	τ (μs)	r_0 (Ω m)	ρ_∞ (Ω m)	α
5	10	5.46	14.268	1.9927	0.14109
5	100	5.40	14.25	1.9809	0.13993
5	440	5.40	14.25	1.9799	0.14002
7	10	5.43	14.22	2.0074	0.13709
7	100	5.40	14.249	1.9803	0.13988
7	440	5.40	14.25	1.98	0.13998
10	10	5.31	14.207	1.9314	0.13446
10	100	5.40	14.251	1.979	0.14022

The sequence of steps is similar to that of section 5.2. Figure 4 presents the results to seven impedivity data, and table 4 presents the results for different values of impedivity and different values of generations:

$$\omega = 2\pi\{100, 464.16, 2154.40, 10^4, 46\,416, 215\,440, 10^6\}\ (\text{rad s}^{-1})$$
$$R = \{2.9578, 3.714, 4.9356, 6.678, 8.7289, 10.641, 12.081\}\ (\Omega\,\text{m})$$
$$I = \{0.630\,25, 1.0202, 1.4974, 1.894, 1.9753, 1.683, 1.2107\}\ (\Omega\,\text{m}).$$

6. Numerical integration for the Kramers–Kronig relation

A numerical integration for the Kramers–Kronig relation was implemented in the following way. Assuming that $N + 1$ are data written as $\{(\omega_k, R_k) \mid k = 1, 2, \ldots, N + 1\}$, where $R_k = \text{Re}\{\rho(\text{j}\omega_k)\}, k = 1, 2, \ldots, N + 1$, then the imaginary part of the impedivity should be obtained by the Kramers–Kronig relation as

$$I_k = \text{Im}\{\rho(\text{j}\omega_k)\} = \frac{2\omega_k}{\pi}\int_0^\infty \frac{\text{Re}\{\rho(\text{j}v)\} - \rho_\infty}{\omega_k^2 - v^2}\,\text{d}v. \tag{13}$$

Four aspects should be considered before the numerical integration of the Kramers–Kronig relation could be done. First, the singularity around ω_k; second, the frequency obtained

$\mathrm{Re}\{\rho(\mathrm{j}\omega_\infty)\} = \rho_\infty$; third, the spectral data to low frequencies; and finally, the number of spectral data.

The singularity could be avoided by rewriting the singularity by partial fractions as follows:

$$\begin{aligned} I_k &= \frac{2}{\pi}\int_0^\infty \langle \mathrm{Re}\{\rho(\mathrm{j}v)\} - \rho_\infty\rangle \left(\frac{1}{\omega_k^2 - v^2}\omega_k\right) \mathrm{d}v \\ &= \frac{2}{\pi}\int_0^\infty \left[\frac{\mathrm{Re}\{\rho(\mathrm{j}v)\} - \rho_\infty}{2}\left(\frac{1}{\omega_k - v} + \frac{1}{\omega_k + v}\right)\right] \mathrm{d}v \\ I_k &= \frac{1}{\pi}\int_0^\infty \frac{\mathrm{Re}\{\rho(\mathrm{j}v)\} - \rho_\infty}{\omega_k + v}\,\mathrm{d}v \\ &\quad + \frac{1}{\pi}\lim_{\delta\omega\to 0}\left\{\int_0^{\omega_k-\delta\omega} \frac{\mathrm{Re}\{\rho(\mathrm{j}v)\} - \rho_\infty}{\omega_k - v}\,\mathrm{d}v + \int_{\omega_k+\delta\omega}^\infty \frac{\mathrm{Re}\{\rho(\mathrm{j}v)\} - \rho_\infty}{\omega_k - v}\,\mathrm{d}v\right\} \end{aligned} \tag{14}$$

Let $\omega_k - \delta\omega = \omega_{k-1}$ and $\omega_k + \delta\omega = \omega_{k+1}$ when the number of points is very big. Then,

$$\begin{aligned} I_k &\cong \frac{1}{\pi}\int_0^\infty \frac{\mathrm{Re}\{\rho(\mathrm{j}v)\} - \rho_\infty}{\omega_k + v}\,\mathrm{d}v \\ &\quad + \frac{1}{\pi}\left\{\int_0^{\omega_{k-1}} \frac{\mathrm{Re}\{\rho(\mathrm{j}v)\} - \rho_\infty}{\omega_k - v}\,\mathrm{d}v + \int_{\omega_{k+1}}^\infty \frac{\mathrm{Re}\{\rho(\mathrm{j}v)\} - \rho_\infty}{\omega_k - v}\,\mathrm{d}v\right\}. \end{aligned} \tag{15}$$

To evaluate the integration between zero and infinity a definition of extra spectral data could be useful: let $\mathrm{Re}\{\rho(\mathrm{j}v)\} = R_{N+1}$ for all $v \geqslant \omega_{N+1}$, and $\mathrm{Re}\{\rho(\mathrm{j}v)\} = R_1$ for all values between zero and ω_1. With extra spectral data (15) should be written as follows:

$$\begin{aligned} I_k &\cong \frac{R_1 - R_{N+1}}{\pi}\left(\int_0^{\omega_1} \frac{1}{\omega_k + v}\,\mathrm{d}v + \int_0^{\omega_1} \frac{1}{\omega_k - v}\,\mathrm{d}v\right) + \frac{1}{\pi}\int_{\omega_1}^{\omega_{N+1}} \frac{\mathrm{Re}\{\rho(\mathrm{j}v)\} - R_{N+1}}{\omega_k + v}\,\mathrm{d}v \\ &\quad + \frac{1}{\pi}\left\{\int_{\omega_1}^{\omega_{k-1}} \frac{\mathrm{Re}\{\rho(\mathrm{j}v)\} - R_{N+1}}{\omega_k - v}\,\mathrm{d}v + \int_{\omega_{k+1}}^{\omega_{N+1}} \frac{\mathrm{Re}\{\rho(\mathrm{j}v)\} - R_{N+1}}{\omega_k - v}\,\mathrm{d}v\right\}. \end{aligned} \tag{16}$$

But $\int_0^{\omega_1} \frac{1}{\omega_k+v}\,\mathrm{d}v + \int_0^{\omega_1} \frac{1}{\omega_k-v}\,\mathrm{d}v = 2\omega_k \int_0^{\omega_1} \frac{1}{\omega_k^2-v^2}\,\mathrm{d}v = \ln\left|\frac{\omega_k-\omega_1}{\omega_k+\omega_1}\right|$, then

$$\begin{aligned} I_k &\cong \frac{(R_1 - R_{N+1})}{\pi}\ln\left|\frac{\omega_k - \omega_1}{\omega_k + \omega_1}\right| + \frac{1}{\pi}\int_{\omega_1}^{\omega_{N+1}} \frac{\mathrm{Re}\{\rho(\mathrm{j}v)\} - R_{N+1}}{\omega_k + v}\,\mathrm{d}v \\ &\quad + \frac{1}{\pi}\left\{\int_{\omega_1}^{\omega_{k-1}} \frac{\mathrm{Re}\{\rho(\mathrm{j}v)\} - R_{N+1}}{\omega_k - v}\,\mathrm{d}v + \int_{\omega_{k+1}}^{\omega_{N+1}} \frac{\mathrm{Re}\{\rho(\mathrm{j}v)\} - R_{N+1}}{\omega_k - v}\,\mathrm{d}v\right\}. \end{aligned} \tag{17}$$

Finally, the numerical integration is possible if $\mathrm{Re}\{\rho(\mathrm{j}v)\}$ is known to all v, but few spectral data are available. To avoid this difficulty many ways are possible but Simpson numerical integration and Maclaurin's formula give the best result.

First, the Simpson numerical integration is studied, and second, the trapezium integration and Maclaurin's formula.

6.1. Simpson numerical integration

Two numerical integrations required are $\int_{\omega_l}^{\omega_{l+2}} \frac{\mathrm{Re}\{\rho(jv)\}-R_{N+1}}{\omega_k - v}\,\mathrm{d}v$ and $\int_{\omega_1}^{\omega_{N+1}} \frac{\mathrm{Re}\{\rho(jv)\}-R_{N+1}}{\omega_k + v}\,\mathrm{d}v$.

Simpson numerical integration is as follows: let $f(x)$ be a real function defined on interval (x_1, x_3), then the Simpson rule is

$$\int_{x_1}^{x_3} f(x)\,\mathrm{d}x = \frac{h}{3}\,[f(x_1) + 4f(x_2) + f\,(x_3)] + O(\xi),$$

where $h = \frac{x_3 - x_1}{2}$ and $O(\xi) = -\frac{h^5}{90} f^{(4)}(\xi)$ is the error for numerical Simpson integration.

Let $f\,(v; \omega_\mathrm{k}) = \frac{\mathrm{Re}\{\rho(\mathrm{j}v)\}-R_{N+1}}{\omega_k - v}$, then

$$\int_{\omega_l}^{\omega_{l+2}} \frac{\mathrm{Re}\{\rho(\mathrm{j}v)\} - R_{N+1}}{\omega_k - v}\,\mathrm{d}v \cong \frac{\omega_{l+2} - \omega_l}{6}[f\,(\omega_l; \omega_\mathrm{k}) + 4f\,(\omega_{l+1}; \omega_\mathrm{k}) + f\,(\omega_{l+2}; \omega_\mathrm{k})]$$

Furthermore, the second integral should be evaluated by the successive application of Simpson. Let $g\,(v; \omega_\mathrm{k}) = \frac{\mathrm{Re}\{\rho(\mathrm{j}v)\}-R_{N+1}}{\omega_k + v}$, then

$$\int_{\omega_1}^{\omega_{N+1}} \frac{\mathrm{Re}\{\rho(\mathrm{j}v)\} - R_{N+1}}{\omega_k + v}\,\mathrm{d}v \cong \sum_{l=1}^{(\frac{N+1}{3})} \frac{\omega_{3l} - \omega_{3l-2}}{6}[g(\omega_{3l-2}; \omega_\mathrm{k}) + 4g(\omega_{3l-1}; \omega_\mathrm{k}) + g(\omega_{3l}; \omega_\mathrm{k})].$$

The Kramers–Kronig numerical integration gives the imaginary part of impedivity obtained by

$$\begin{aligned} I_k \cong\ & \frac{(R_1 - R_{N+1})}{\pi} \ln\left|\frac{\omega_k - \omega_1}{\omega_k + \omega_1}\right| \\ & + \frac{1}{\pi} \sum_{l=1}^{(\frac{N+1}{3})} \frac{\omega_{3l} - \omega_{3l-2}}{6}\,[g\,(\omega_{3l-2}; \omega_\mathrm{k}) + 4g\,(\omega_{3l-1}; \omega_\mathrm{k}) + g\,(\omega_{3l}; \omega_\mathrm{k})] \\ & + \frac{1}{\pi} \sum_{l=1}^{(\frac{k-1}{3})} \frac{\omega_{3l} - \omega_{3l-2}}{6}\,[f\,(\omega_{3l-2}; \omega_\mathrm{k}) + 4f\,(\omega_{3l-1}; \omega_\mathrm{k}) + f\,(\omega_{3l}; \omega_\mathrm{k})] \\ & + \frac{1}{\pi} \sum_{l=k+1}^{(\frac{N+1}{3})} \frac{\omega_{3l} - \omega_{3l-2}}{6}\,[f\,(\omega_{3l-2}; \omega_\mathrm{k}) + 4f\,(\omega_{3l-1}; \omega_\mathrm{k}) + f\,(\omega_{3l}; \omega_\mathrm{k})], \end{aligned} \tag{18}$$

where $f\,(v; \omega_\mathrm{k}) = \frac{\mathrm{Re}\{\rho(\mathrm{j}v)\}-R_{N+1}}{\omega_k - v}$ and $g\,(v; \omega_\mathrm{k}) = \frac{\mathrm{Re}\{\rho(\mathrm{j}v)\}-R_{N+1}}{\omega_k + v}$.

6.2. Trapezium numerical integration

A trapezium numerical integration should be implemented based on Maclaurin's formula (Ohta and Ishida 1988).

Trapezium numerical integration is as follows: let $f(x)$ be a real function defined on the interval (x_1, x_2), then the Simpson rule is

$$\int_{x_1}^{x_2} f(x)\,\mathrm{d}x = \frac{h}{2}\,[f(x_1) + f(x_2)] + O(\xi),$$

where, $h = \frac{x_2 - x_1}{2}$ and $O(\xi) = -\frac{h^3}{12} f^{(3)}(\xi)$ is the error for the numerical trapezium integration.

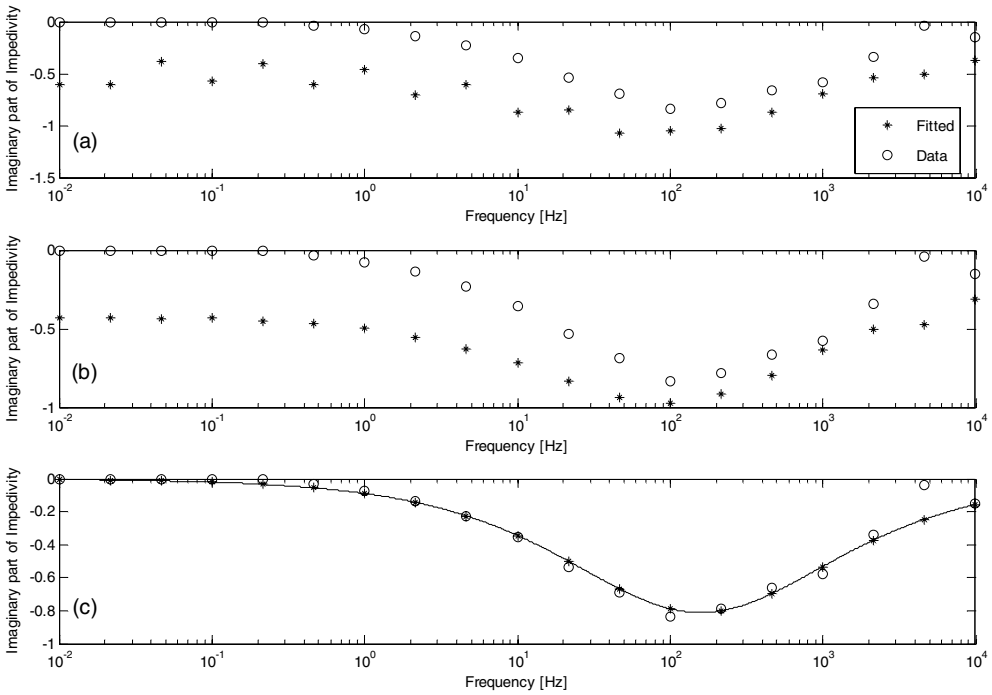

Figure 5. The imaginary part of impedivity obtained by (a) numerical integration for the Kramers–Kronig relation by Simpson's rule, (b) numerical integration for the Kramers–Kronig relation by trapezium formula (based on Maclaurin's formula) and (c) proposed algorithm.

Then, the Kramers–Kronig numerical integration, the imaginary part of the impedivity, should be obtained by

$$I_k \cong \frac{(R_1 - R_{N+1})}{\pi} \ln\left|\frac{\omega_k - \omega_1}{\omega_k + \omega_1}\right| + \frac{1}{\pi}\sum_{l=1}^{\left(\frac{N+1}{2}\right)} \frac{\omega_{2l} - \omega_{2l-1}}{4}[g\,(\omega_{2l-1};\omega_{\mathrm{k}}) + g\,(\omega_{2l};\omega_{\mathrm{k}})]$$
$$+ \frac{1}{\pi}\sum_{l=1}^{\left(\frac{k-1}{2}\right)} \frac{\omega_{2l} - \omega_{2l-1}}{4}[f\,(\omega_{2l-1};\omega_{\mathrm{k}}) + f\,(\omega_{2l};\omega_{\mathrm{k}})]$$
$$+ \frac{1}{\pi}\sum_{l=k+1}^{\left(\frac{N+1}{2}\right)} \frac{\omega_{2l} - \omega_{2l-1}}{4}[f\,(\omega_{2l-1};\omega_{\mathrm{k}}) + f\,(\omega_{2l};\omega_{\mathrm{k}})], \tag{19}$$

where $f\,(v;\omega_{\mathrm{k}}) = \frac{\mathrm{Re}\{\rho(\mathrm{j}v)\} - R_{N+1}}{\omega_k - v}$ and $g\,(v;\omega_{\mathrm{k}}) = \frac{\mathrm{Re}\{\rho(\mathrm{j}v)\} - R_{N+1}}{\omega_k + v}$.

7. Comparison among numerical integrations for the Kramers–Kronig relation and the proposed algorithm

To compare different numerical integrations for the Kramers–Kronig relation in the proposed algorithm, numerical resistivity data are required; in this case, using the Cole–Cole relation. Various sets of spectral data were obtained using the Cole–Cole relation and experimental data. The comparison of numerical integration and the proposed algorithm is shown in table 5 and figure 5.

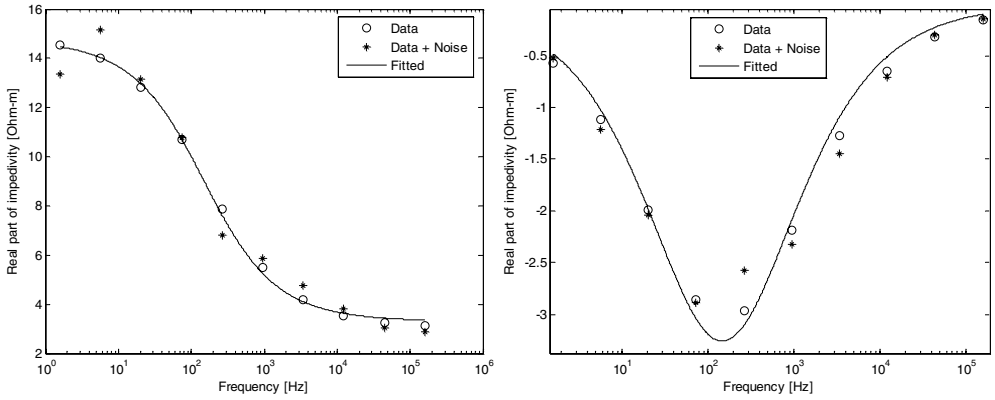

Figure 6. Shows the adjustment of data with 30% random additive noise, where (a) is the real part of the impedivity and (b) the imaginary part of the impedivity.

Table 5. Comparison among numerical integration for the Kramers–Kronig relation and the proposed algorithm.

		Kramers–Kronig numerical integration for Simpson's rule		Kramers–Kronig numerical integration for Maclaurin's formula		Proposed algorithm	
Data source	Spectral points	RMS error[a] ($\times 10^{-3}$)	Elapsed time (ms)	RMS error[a] ($\times 10^{-3}$)	Elapsed time (ms)	RMS error[a] ($\times 10^{-3}$)	Elapsed time (s)
Cole–Cole model:	5	12098	31	31588	15	3	4.2
$\rho(j\omega) = 20 +$	25	1352	31	1131	16	3	5.0
$\frac{18}{1+\frac{j\omega}{20000\pi}}$ (Ω m)	125	224	125	201	31	3	17.5
	625	43	2250	45	218	3	60.9
	3125	9	56313	14	5156	3	277.5
Jaggar and Fell (1988)	19	417	31	343	16	54	9565.7

[a] RMS $= \sqrt{\frac{1}{N+1}\sum_k \langle \mathrm{Im}\{\rho(j\omega_k)\} - I_k)^2}$

Table 6. Inversion of data with additive noise.

	Real parameters				Inversion values			
Noise (%)	ρ_0 (ms)	ρ_0 (Ω m)	ρ_∞ (Ω m)	α	ρ_0 (ms)	ρ_0 (Ω m)	ρ_∞ (Ω m)	α
0	1	15	3	0.4	0.999	14.995	3.003	0.399
5	1	15	3	0.4	1.003	15.118	2.982	0.408
10	1	15	3	0.4	0.910	15.121	3.042	0.380
30	1	15	3	0.4	1.075	14.786	3.297	0.343

8. Noise immunity

The proposed algorithm yields excellent noise immunity. The experimental data were simulated with additive random noise up to 30% of the maximum value of the real part

of the electrical impedivity spectrum. In figure 6 the result of the simulation is shown, where the star represents the noise data, circles represent the data without noise and the solid line represents the adjusted curve.

Table 6 presents the results of the noise simulation.

9. Conclusion

A new algorithm is presented to search the imaginary part of the impedivity from the real part. The algorithm proposed enables data to be fitted to the Cole–Cole equation using only the real part of the electrical impedivity spectrum, based upon the Xiang inversion technique and a genetic algorithm optimization. The additive random noise immunity is very high. Cole–Cole parameters can be obtained with up to 30% of additive noise. The algorithm converges fast, and it has very good stability and high precision. It gives a good parameter estimation. The proposed algorithm was compared with different numerical integrations of the Kramers–Kronig relation and the result shows that this algorithm is the best.

When the α Cole–Cole parameter is zero, the Debye direct inversion may give a good approximation. However, the use of a genetic algorithm allows a better search of the imaginary part of the impedivity, the Cole–Cole parameters and also good noise immunity.

The use of only a few spectral data of the real part of the impedivity enables the genetic algorithm to search a minimum error with few generations and populations, but when a large amount of data are used, the number of generations and the time of calculation increase.

The theory of the interpretation of biological impedivity may be of intrinsic interest to electronic engineers and medical physicists. The determination of the Cole–Cole parameters has been of considerable interest for many applications: neoplasical screening, electrical bioimpedance, geophysics and material science.

Acknowledgment

The financial support of the 'Vicerrectoría de Investigación y Extensión de la Universidad Industrial de Santander (VIE-UIS)', 'COLCIENCIAS' and 'Consejo de Desarrollo Científico Humanístico y Tecnológico (CDCHT)' is gratefully acknowledged.

References

Ackmann J and Seitz M 1984 Methods of complex impedance measurements in biologic tissue *Crit. Rev. Biomed. Eng.* **11** 281–311

Brown B, Tidy J, Boston K, Blackett A, Smallwood R and Sharp F 2000 Relation between tissue structure and imposed electrical current flow in cervical neoplasia *Lancet* **355** 892–5

Cao Z, Chang Y and Luo Y 2005 Inversion study of spectral induced polarization based on improved genetic algorithm *Progress in Electromagnetic Research Symposium 2005 (Hangzhou, China, 22–26 August 2005)*

Cardona M 1969 *Modulation Spectroscopy* (New York: Academic) pp 9–10

Cole K S 1940 Permeability and impermeability of cell membranes fot ions *Cold Spring Harb. Symp. Quant. Biol.* **8** 110–22

Cole K and Cole R 1941 Dispersion and absorption in dielectrics *J. Chem. Phys.* **9** 341–51

Jaggar S and Fell P 1988 Forward and inverse Cole–Cole modelling in the analysis of frequency domain electrical impedance data *Explor. Geophys.* **19** 463–70

Kramers H A 1927 La diffusion de la lumiere par les atomes *Atti Cong. Intern. Fisica (Transactions of Volta Centenary Congress) Como* vol 2 pp 545–57

Kronig R 1926 On the theory of the dispersion of x-rays *J. Opt. Soc. Am.* **12** 547–57

Miranda D, Barrero J and Hecheverri J 2007 *Estudio para la detección temprana del cáncer de cuello uterino* (Colombia: SiC Editorial) pp 96–8

Ohta K and Ishida H 1988 Comparison among several numerical integration methods for Kramers–Kronig transformation *Appl. Spectrosc.* **42** 952–7

Schwan H 1994 Electrical properties of tissues and cell suspensions: mechanism and models *IEEE Proc. EMBS* pp 70a–71a

Ward L, Essex T and Cornish B 2006 Determination of Cole parameters in multiple frequency bioelectrical impedance analysis using only the measurement of impedances *Phyiol. Meas.* **27** 839–50

Xiang J, Cheng D, Schlindwein F and Jones N 2003 On the adequacy of identified Cole–Cole models *Comput. Geosci.* **29** 647–54

Xiang J, Jones N, Cheng D and Schlindwein F 2001 Direct inversion of the apparent complex-resistivity spectrum *Geophysics* **66** 1399–404